# MIT Open Access Articles

## Using nature's blueprint to expand catalysis with Earth-abundant metals

**Massachusetts Institute of Technology**

# Using nature's blueprint to expand catalysis with Earth-abundant metals

R. Morris Bullock,* Jingguang G. Chen,* Laura Gagliardi,* Paul J. Chirik, Omar K. Farha, Christopher H. Hendon, Christopher W. Jones, John A. Keith, Jerzy Klosin, Shelley D. Minteer, Robert H. Morris, Alexander T. Radosevich, Thomas B. Rauchfuss, Neil A. Strotman, Aleksandra Vojvodic, Thomas R. Ward, Jenny Y. Yang, and Yogesh Surendranath*

(RMB) Center for Molecular Electrocatalysis, Pacific Northwest National Laboratory, Richland, WA 99352, United States
(JGC) Department of Chemical Engineering, Columbia University, New York, New York 10027, United States; Chemistry Division, Brookhaven National Laboratory, Upton, New York 11973, United States
(LG) Department of Chemistry, Minnesota Supercomputing Institute, and Chemical Theory Center, University of Minnesota, Minneapolis, Minnesota 55455, United States
(PJC) Department of Chemistry, Princeton University, Princeton, New Jersey 08544, United States
(OKF) Department of Chemistry and Chemical and Biological Engineering, Northwestern University, 2145 Sheridan Road, Evanston, Illinois 60208, United States
(CHH) Department of Chemistry and Biochemistry, University of Oregon, Eugene, OR, 97403, United States
(CWJ) School of Chemical & Biomolecular Engineering, Georgia Institute of Technology, Atlanta, GA 30332, United States
(JAK) Department of Chemical and Petroleum Engineering University of Pittsburgh, 3700 O'Hara Street, Pittsburgh, PA 15261, United States
(JK) Core R&D, The Dow Chemical Company, Midland, Michigan 48674, United States
(SM) Department of Chemistry, University of Utah, 315 South 1400 East, Salt Lake City, Utah 84112, United States
(RHM) Department of Chemistry, University of Toronto, 80 St. George Street Toronto, Ontario M5S 3H6, Canada
(ATR) Department of Chemistry, Massachusetts Institute of Technology, Cambridge, Massachusetts, 02139, United States
(TBR) School of Chemical Sciences, University of Illinois, Urbana, Illinois 61801, United States
(NAS) Process Research and Development, Merck & Co., Inc., Rahway, NJ 07065, United States
(AV) Department of Chemical & Biomolecular Engineering, University of Pennsylvania, Philadelphia, PA 19104, United States
(TRW) Department of Chemistry, University of Basel, BPR1096, Mattenstrasse 24a, CH-4058 Basel, Switzerland
(JYY) Department of Chemistry, University of California, Irvine, California 92697, United States
(YS) Department of Chemistry, Massachusetts Institute of Technology, Cambridge, Massachusetts 02139, United States

**Abstract:** Numerous redox transformations that are essential to life are catalyzed by metalloenzymes that feature an earth-abundant metal. In contrast, platinum-group metals have been the cornerstone of many industrial catalytic reactions for decades, providing high activity, thermal stability and tolerance to chemical poisons. We assert that nature's blueprint provides the fundamental principles for vastly expanding the use of abundant metals in catalysis. We highlight the key physical properties of abundant metals that distinguish them from precious metals, and we look to nature to understand how the inherent attributes of abundant metals can be embraced to produce unique, highly efficient catalysts for reactions crucial to the sustainable production and transformation of fuels and chemicals.

Catalysis has had a transformative impact on society, playing a decisive role in the production of modern materials we use daily, medicines to keep us healthy, and fuels for transportation. Most of the key chemical reactions essential to our contemporary lifestyle are catalyzed by transition metals (TMs). The terrestrial abundance of TMs varies dramatically: the 1st row (3d) metals of the transition series in the periodic table, as well as the early 2nd row (4d) and 3rd row (5d) metals, are relatively abundant, whereas the platinum groups metals (PGMs) that comprise the mid to late portion of the 2nd and 3rd row have dramatically lower crustal abundance (Figure 1).(*1*) In this perspective review, we highlight frontier opportunities for designing and enabling new catalysts based on earth-abundant metals (EAMs), with an emphasis on redox reactions crucial to the sustainable production and transformation of fuels and chemicals.



**Figure 1.** Definition of different groups of transition metals. PGMs include Ru, Rh, Pd, Os, Ir, and Pt. The broader term, precious metals, includes PGMs, along with Re, Au, and Ag. EAMs (sometimes referred to as base metals) include all other transition metals. (Tc is shown, but is radioactive and unstable.) The height of the pillar for each metal indicates the crustal abundance, on a log scale; the values range from 5.6% (Fe) to ~0.001 ppm (Rh, Ir). The black bar on each metal shows (also on a log scale) the relative amount of $CO_2$ produced through mining and purification for each metal(*2*) which is markedly larger for PGMs than for EAMs.

Many redox transformations(*3*) that are essential to life are catalyzed by EAMs in nature. Because biological organisms must accumulate metals from their surroundings, evolution selected the EAMs exclusively in biological catalysis. Indeed, there are no known native biological

catalysts that use a PGM. Consequently, metalloenzymes provide an expansive existence proof that EAMs catalyze complex redox transformations. A tri-Cu active site in the laccase enzyme(*4, 5*) reduces $O_2$ to $H_2O$, a key cathodic reaction in fuel cells; a cluster containing Fe and Mo reduces $N_2$ to $NH_3$ in nitrogenase;(*6*) a dinuclear Ni active site catalyzes the CO insertion reaction in acetyl-CoA synthase (Figure 2 top left); enzymes containing Ni-Fe organometallic complexes carry out the reversible interconversion of $H_2$ and $H^+$ in hydrogenase(*7*) (Figure 2 middle left); a Mn-Ca cluster catalyzes the oxidation of water to $O_2$ in photosystem II(*8*) (Figure 2 bottom left); the selective oxidation of methane to methanol occurs at the dinuclear Fe active site in methane monooxygenase;(*9*) and diverse C-H functionalization reactions are catalyzed by Fe-S cluster active sites in radical *S*-adenosylmethionine (SAM) enzymes.(*10*) All of these transformations involve multi-electron redox reactions, and most require precise control of the delivery or removal of protons.

In contrast to the extensive use of EAMs in Nature, PGMs have historically been the cornerstone of many industrial catalytic reactions for decades, owing to their high catalytic activity, thermal stability and their tolerance to chemical poisons. Pd-catalyzed cross-coupling catalysts that form C-C bonds(*11*) have broad utility and tremendous versatility in pharmaceutical, electronic, and materials applications. A second wave of Pd-catalyzed cross-coupling chemistry, largely driven by the work of Buchwald and Hartwig, has given rise to powerful methods for C-N, C-S, and C-O bond-forming reactions that are widely used.(*12*) Rh-based complexes catalyze the CO insertion reaction, hydroformylation(*13*) (Figure 2 top right); Pt is the prototypical catalyst for hydrogen production(*14*) and oxidation (Figure 2 middle right); Ir oxide catalyzes oxidation of water to $O_2$(*15*) in PEM electrolyzers (Figure 2 bottom right); C-H oxidation and functionalization reactions have been extensively developed using Pd catalysts;(*16*) selective hydrogenation reactions required in oil refining and fine chemical synthesis routinely employ PGM catalysts; and the three-way catalyst in catalytic converters used daily in hundreds of millions of cars requires Pt, Rh and Pd.
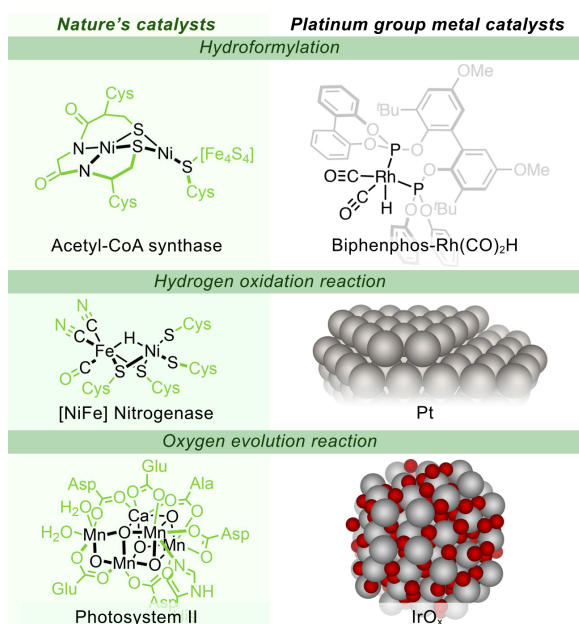


**Figure 2.** Many of the transformations carried out by enzymatic EAM catalysts are carried out in the chemical industry using PGM catalysts.

EAM catalysts are attractive for many reasons. The "terawatt challenge"(*17*) for global energy demand highlights the need to consider the scalability of catalytic materials for sustainable energy conversions. The crustal abundance of EAMs exceeds those of PGMs by a factor of $10^4$ or greater (Figure 1), leading to costs that differ by similar ratios. Costs are influenced both by abundance and production rate.(*18*) The price (Nov. 2019) of a mole of Rh reached >$15,000 (US $), whereas the cost of most EAMs is typically <$2 per mole (though for many catalytic reactions, the metal cost constitutes only a small fraction of the overall process cost; in the synthesis of pharmaceutical products, the cost of chiral ligands can substantially exceed that of the metal). Prices of PGMs are much more volatile than those of EAMs. Moreover, EAMs generally have lower biological toxicity,(*19*) permitting higher levels of residual EAMs than PGMs in pharmaceutical products.(*20*) Lastly, the high abundance of EAMs generally leads to a lower environmental footprint associated with their mining and purification relative to PGMs. For example, the production of one kg of Rh generates >35,000 kg equivalents of $CO_2$, while one kg of Ni produces only 6.5 kg equivalents of $CO_2$ (Figure 1, black bars).(*2*)

Given the appealing attributes of EAMs noted above, one can ask why PGMs continue to be so prevalent in many industrial catalytic processes. The specific reasons vary, depending on each catalytic application. In general, the requirement for effective integration of a catalyst into an overall process often places stringent constraints on the choice of the catalyst. For example, in a fuel cell, the requirement for fast ion conductivity in Nafion requires an acidic pH, constraining the choice of catalysts to corrosion-resistant PGMs. Likewise, the requirement for high temperature operations in catalytic converters places stringent requirements on durability, constraining viable replacement of PGMs. In addition, the high capital and energy cost of complex downstream separations imposes a constraint on the minimum selectivity of catalytic processes, and this consideration may dominate relative to the cost and environmental footprint of the metal catalyst itself. These factors motivate the emphasis on the development of EAM catalysts in tandem with new processes that can circumvent the constraints of current catalytic technologies.

EAM catalysts are currently successfully used in several major industrial processes. The Haber-Bosch reaction, which converts $N_2$ to ammonia, uses an Fe-based catalyst, despite the higher performance of a Ru-based analogue.(*21*) Hydrogenation of CO to methanol is carried out using a Cu/Zn-based catalyst. Hydrogen is produced from water in commercial electrolyzers under basic conditions using Ni/Fe-based catalysts. Olefin oligomerization and polymerizations are carried out worldwide on a tremendous scale using EAMs, dominated by Ti, Zr, and Cr catalysts. Terephthalic acid is produced on a large scale through oxidation of *p*-xylene using Co and Mn catalysts. Some industrial processes are catalyzed by both PGMs and EAMs. For example, hydroformylation is conducted using either Co- or Rh-based catalysts,(*13*) and propane dehydrogenation is carried out on either Pt- or Cr-based catalysts.(*22*) Despite these examples, it remains clear that the scope of EAM catalysis is dramatically limited compared to the remarkable diversity of transformations catalyzed by EAMs in nature.

Whereas biology provides an invaluable (though sometimes inscrutable) guide to the broadened implementation of EAMs, industrial catalysis often requires substrates, reactions, and reaction conditions quite different from those in biology; PGM catalysts proliferate in this arena. For example, alkenes, which are derived from petroleum, are processed quite differently by enzymes compared to industrial catalysts. With the notable exception of Cu-based ethylene-sensor proteins,(*23*) metal-alkene complexes are unknown in nature, though transfer hydrogenations of C=C bonds are catalyzed by a family of biocatalysts, ene-reductases.(*24*) In stark contrast, industrial catalysis of alkenes includes polymerization, carbonylation, and metathesis; analogues

of these processes are absent from the biocatalysis repertoire. Instead, alkenes are often processed in natural systems by attacking weakened allylic C-H bonds using iron-oxo-based radicals.(*25*) Considering the diversity of catalysis performed by biological systems, a central challenge revolves around coaxing biological macromolecules into displaying entirely abiotic reactivity/selectivity/stability characteristics that have traditionally been the domain of PGM-based catalysts. A daunting challenge in designing bio-inspired catalysts is to identify and replicate only the parts of the metalloenzyme structure (first, second, or outer coordination sphere) that are thought to be required for catalytic activity, recognizing that while biological reaction networks must maintain life, their catalytic functionality may be accessible from synthetically simpler structures. Replicating the active site is necessary but not sufficient for achieving catalysis comparable to that found in enzymes, as dynamics and conformational changes often exert a large influence on enzymatic catalysis.(*26*)

The considerations discussed above have fueled burgeoning interest in developing new EAM-based catalysts. We assert that this endeavor is best advanced by establishing the fundamental science of EAMs that embraces their unique physical properties and resultant catalytic activities. Herein, we put forward the premise that nature's blueprint provides the fundamental principles for vastly expanding the use of EAMs in catalysis. We highlight the key physical properties of EAMs that distinguish their reactivity from those of PGMs, and then seek to understand how the inherent attributes of EAMs can be embraced, leading to unique, highly efficient catalysis. Building on that foundation, we identify compelling opportunities for the increased use of EAMs in enzymatic, molecular, and heterogeneous catalysis.

## The origins of divergent reactivity between EAMs and PGMs

*Electronic Structure*. The distinctive reactivity profiles of EAMs relative to PGMs originate from fundamental differences arising from periodic trends of the elements.(*27*) In particular, 3d orbitals extend to a lesser extent beyond the 3s and 3p orbitals,(*28*) leading to attenuated orbital overlap with bonding partners, relative to the corresponding 4d and 5d counterparts. This overlap deficit dramatically impacts the electronic structure of 3d metal-based catalysts. For molecular TM complexes, the overlap deficit leads to more ionic character in metal-ligand bonds, and a small frontier d-orbital splitting (Figure 3 top), stabilizing high-spin electronic configurations. High spin configurations are extremely rare(*29, 30*) among 4d and 5d TM complexes owing to their much higher frontier orbital splitting energies (Figure 3 top). Similar phenomena are observed for extended solids: attenuated orbital overlap between 3d metal atoms leads to a diminished spread in the d-band energies and a corresponding increase in the d-band center of 3d metals relative to the 4d and 5d counterparts (Figure 3 top). The prevalence of high spin electronic configurations amongst 3d TMs has important implications for reactivity.(*31*) Homogeneous catalysts of PGMs typically cycle through two-electron processes, including familiar examples of oxidative addition/reductive elimination of $Rh^I/Rh^{III}$ and $Pd^0/Pd^{II}$. In contrast, 3d TM complexes more readily engage in single-electron bond activation reactions, including M-X bond homolysis. Additionally, the availability of multiple spin states among EAMs can lead to multi-state acceleration of certain reactions.

*Thermochemistry*. The differences in the electronic structures of EAMs and PGMs are manifested in the thermochemistry of interactions of metals with ligands, reactants, products and intermediates. The classical Sabatier principle states that an optimal catalyst should bind intermediates neither too strongly nor too weakly, essentially a "Goldilocks" effect.(*21*) In general, bonding to 3d TMs in molecular complexes is weaker relative to 4d/5d TM centers with the same

ancillary ligand environment. For example, the bond dissociation energies of the M-H bond in MH($\eta^5$-C$_5$H$_5$)(CO)$_2$ are 68, (*32*) 77(*32*) and ≥82(*33*) kcal/mol for Fe, Ru, and Os, respectively; for MH(CO)$_5$ the values are 68 and 75 kcal/mol for Mn and Re, respectively.(*34*) Additionally, the greater extension of the d-orbitals of the 2$^{nd}$ and 3$^{rd}$ TMs also provides for greater back-bonding interactions with π-accepting ligands, such as CO and olefins, increasing their binding strength. Intermediates bearing such ligands are critical in a number of industrially important processes, such as hydroformylation.

The differences in metal bonding thermochemistry are also mirrored in changes in the reduction potentials of metal ions. PGMs are commonly referred to as noble because of their resistance to oxidation, a reflection of their much higher reduction potentials and lower O-atom affinities of 4d and 5d metals (Figure 3 middle, black) relative to 3d TMs (Figure 3 middle, blue). For example, whereas the Pt$^{II/0}$ and Pd$^{II/0}$ reduction potentials are 1.18 and 0.951 V, respectively, vs. the standard hydrogen electrode (SHE), the corresponding Ni$^{II/0}$ reduction potential, -0.26 V, is lower by more than a volt. Likewise, Pt(111) and Pd(111) surfaces have a O-atom affinity of ~0.5 eV (12 kcal/mol) whereas Ni(111) surfaces have an O-atom affinity of ~4 eV (92 kcal/mol) (Figure 3). Consequently, early TMs, including 4d/5d TMs, display reduction potentials that are much less positive, and oxygen affinities that are greater, compared to PGMs. Since these baseline reduction potentials correspond to interconversion of the metallic solid and aquated metal ions, they are dramatically influenced by the coordination, electrostatic, and hydrogen bonding environment of the metal center.(*35*) Because of these effects, the active site EAMs in metalloenzymes span a wide range of potentials(*3*) that differ dramatically from their baseline values. Similar potential ranges can be accessible through changes in the coordination environment of synthetic coordination compounds.(*36*) The differences in reduction potential between EAMs and PGMs are of central importance in electrocatalysis, where electron flow drives the conversion of reactants to products. For example, the high M$^{II/0}$ potential of Pt allows it to remain in the metallic state at the high potentials of oxygen reduction catalysis in fuels cells, making it the only currently viable, corrosion-resistant cathode catalyst for polymer electrolyte membrane fuel cells. To achieve similar feats, enzymes, including multi-copper oxidases, laccases(*4, 5*) and cytochrome *c* oxidase,(*37*) use an ensemble of metal centers organized within the protein environment that dramatically alters their redox properties and oxophilicities.
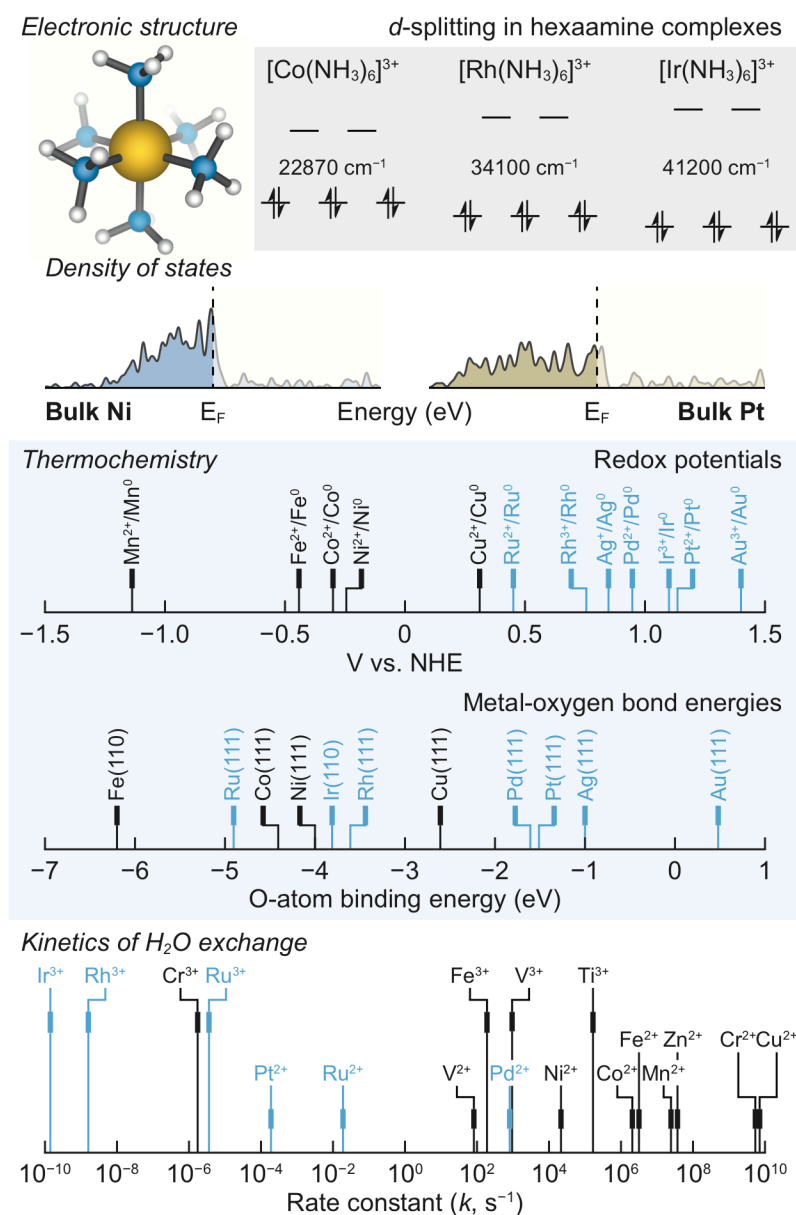
**Figure 3.** Physical properties of EAMs vs. PGMs, illustrating substantial differences that lead to divergent reactivity that can be exploited in catalysis. Data is from Refs. (*1*), (*38*) and (*39*)

*Kinetics*. Owing to their weaker metal-ligand bonds, complexes of the 3d metals are much more labile than their 4d and 5d counterparts (Figure 3 bottom). The rate accelerations can be dramatic – exchange of a water ligand on a high-spin Fe(III) center is $10^8$ faster than on Ru(III).(*39*) We emphasize that lability is a kinetic phenomenon; many labile complexes are thermodynamically stable. Though typically viewed as an impediment to understanding catalytic reactivity, the higher lability of EAMs can, in principle, be beneficial for catalysis. Turnover frequencies are often strongly influenced by the rates of association and dissociation of reactants and products, a manifestation of the Sabatier principle.(*21*) Thus, the inherently higher rate of ligand exchange on the 3d TMs offers the opportunity for rapid catalysis. Two key properties sought are kinetic stability of the metal-supporting ligand ensemble and labile coordination sites

with appropriate affinities for substrates. The challenge arises from the fact that lability of EAMs can also lead to the rapid exchange of supporting ligands that tune the local electronic structure and reaction environment of the metal center. To circumvent problems with lability in molecular complexes, polydentate ligands are often employed to strongly sequester the metal ion while preserving one or more coordination sites for catalysis. Consequently, tridentate or tetradentate ligands are ubiquitous in catalysis by synthetic 3d TMs relative to PGMs, to overcome the inherent differences in lability relative to PGMs. The premier examples of multidentate ligands in biocatalysis are porphyrins, where four metal-nitrogen bonds confer substantial kinetic inertness. Two key properties sought are kinetic stability of the metal-supporting ligand ensemble while preserving axial sites for catalytic reactivity.

In extended solids, the kinetics of substitution at EAMs also play a central role in the longevity of catalysts. The weaker M-lattice bonding in mid to late 3d metal and metal oxide materials contributes to their high propensity to sinter, restructure, become amorphous, and corrode under catalytic conditions, relative to 4d and 5d analogues. A richer understanding of how to control metal lability in extended solids is essential for creating robust EAM catalysts, particularly for harsh reaction environments.

*Computational insights*. Much of our physical understanding of EAMs has been enhanced through consistent benchmarking between experiment and theory. A comprehensive understanding of EAM reactivity will require a refined understanding of electronic structure, thermochemistry, and kinetics. Yet, current theoretical tools that are effective at modeling multi-configurational electronic structure commonplace amongst EAMs are often ineffective for predicting thermochemical and kinetic properties.[40] This impasse results from the enormous computational expense requisite in calculating properties of EAMs that reside in shallow potential energy wells with a diversity of available spin configurations.

Widely used density functional theory (DFT) has strengths and weaknesses, and both are highlighted in modeling catalysis by EAMs. In some cases, trends can be identified readily using simple basis sets and commonly-used functionals. Often complementing experimental results, theoretical studies can identify rate-determining steps, assign vibrational bands, and determine redox potentials. Useful thermochemical predictions of energies can often be obtained, even if specific spin states may not be easily determined reliably. Spin-transitions and d-orbital splitting of EAMs are difficult to treat because states that are very similar in energy occur frequently with EAMs.

Machine learning (ML)-based methods have generated enormous recent interest in computational analysis of catalysis.[41] In a typical application of ML, large datasets (often results from thousands of DFT calculations) are used for statistical regression analyses with ML methods to identify the most accurately parametrized model for the dataset. A well-trained ML model should successfully interpolate within the chemical/materials space of the training data and be useful for screening molecular/material properties for hypothetical homogeneous[42, 43] and/or heterogeneous[44, 45] catalyst active sites across larger regions of chemical and materials space than is accessible with DFT calculations alone. Complementary to ML approaches, theoretical schemes such as alchemical perturbation DFT allow rapid screening of adsorbate binding energies[46] with minimal pre-calculated reference data and low computational cost.

**Emerging opportunities for catalytic reactivity of EAMs**

Recent progress in the design of EAM catalysts demonstrates their potential in many reactions that traditionally use PGMs, though they often fall short of the performance of PGM catalysts on

one or more benchmarks:(*47*) activity, selectivity, lifetime, or energy efficiency. Yet, EAM-based enzymes have evolved in nature to facilitate an impressively diverse array of reactions. We assert that nature's blueprint provides invaluable guidance for frontier areas of exploration in EAM catalysis that leverages the inherent electronic structure, thermodynamic, and kinetic characteristics of EAMs. We discuss below how to use biologically-inspired approaches to design EAM catalysts with enhanced performance in the context of enzymatic, molecular and heterogeneous reactivity.

*Enzymatic catalysis*

Biological catalysts with transition metal active sites feature exclusively EAMs; a central challenge revolves around modifying enzymes to display abiotic functions (Figure 4).
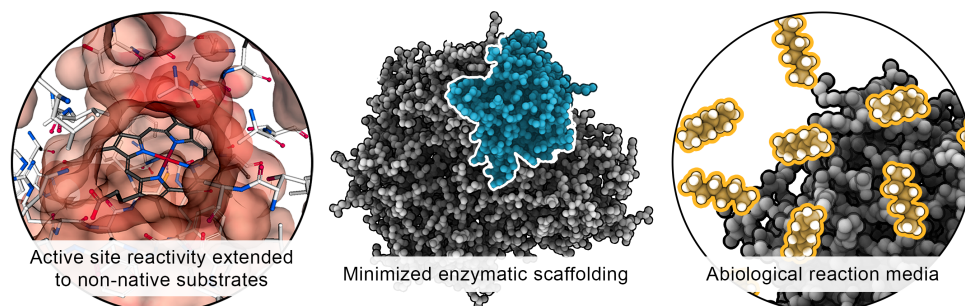


Active site reactivity extended to non-native substrates

Minimized enzymatic scaffolding

Abiological reaction media

**Figure 4.** The utility of enzymatic catalysis can be enhanced by expanding active site reactivity to abiotic substrates, minimizing the enzymatic scaffolding, and enabling operation in non-physiological reaction environments.

Many metalloenzymes display promiscuous activities,(*48*) a feature that provides a diversity of reactivity for the discovery of abiotic enzymatic catalysis. There has been increasing recognition that biological cofactors featuring EAMs are active, albeit at a low level, for a wide array of abiotic transformations that are commonly carried out by synthetic PGM-based catalysts. For example, carbene insertion reactions, which enable the rapid elaboration of simple organic feedstocks into fine and pharmaceutical chemicals, are catalyzed efficiently by synthetic Rh-based catalysts.(*49*) Remarkably, many native hemoproteins also display low-level activity for these same reactions, and directed evolution of these enzymes has led to a family of biocatalysts(*50*) with excellent activity and selectivity for carbene insertion into C-H, N-H, and Si-H bonds. The activity and selectivity of these evolved metalloproteins now rival and even exceed that of Rh-based catalysts. Outstanding recent progress(*51*) showed that hemoproteins can be repurposed to catalyze carbon-carbon bond formation by insertion of a carbene, rather than oxygen, into a C-H bond, a reaction traditionally dominated by PGMs.(*52*) Implementing the blueprint from nature requires precise control of the local environment by modifying the active site to bind an abiotic reactant such as a carbene, while minimizing the binding of the native substrate (i.e., $O_2$) with exquisite selectivity.(*53*) The fundamental workflow of protein engineering – identifying promiscuous reactivity for abiotic substrates, then using protein-engineering tools to maximize performance – serves as a valuable blueprint for further advances in catalysis of abiotic reactions. Continued progress to expand the palette of enzymatic catalysis will benefit from the development of new methods for identifying enzyme candidates and strategies for accelerating directed evolution and selection of high-performance mutant enzymes.

The macromolecular scaffolds that house EAM active sites in enzymes are critical to their function, but invariably afford high-molecular weight catalysts. For commodity scale catalysis, the density of active sites is a critical determinant of space-time yield, imposing constraints on the overall performance. In some cases, subunits of enzymes can be discarded without dramatically lowering catalytic efficiency, suggesting that there is ample opportunity for enhancing active site density without necessarily decreasing the turnover frequency or selectivity of each site. In other cases, mutation of a single amino acid remote from the active site can dramatically alter catalytic performance.(54) Reliable methods for discriminating the portions of the enzyme scaffold that are essential for catalysis from those that are not necessary will facilitate the wider use of enzymatic EAM catalysis for large-scale industrial catalysis.

Many abiotic reactions of critical importance are ideally performed under conditions (temperature, pressure, pH) that are far removed from the mild conditions of biology. For example, catalysts in fuel cells and electrolyzers often operate at the extremes of pH to facilitate ion conduction, and many heterogeneous catalysts operate at elevated temperatures to enhance the reaction rate and facilitate heat integration. Biological systems offer opportunities for adapting enzyme catalysis to extreme reaction conditions. In particular, thermophilic archaea sustain life processes at temperatures exceeding 100 °C and at extremes of pH.(55) It has long been recognized that some enzymes display enhanced catalytic activity in organic solvents,(56) yet there remains limited fundamental understanding of the characteristics of enzymes that engender persistent activity under these conditions. Additionally, whereas abiotic reactivity modes can be screened using abiotic reagents, screening for enzymatic performance under abiotic reaction conditions is more difficult because the biological replication machinery operates within a narrow domain of conditions. Strategies for driving directed evolution within extremophile hosts, and a deeper understanding of the factors that contribute to protein stability, provide plentiful opportunities for extending the rich EAM catalytic reactivity of enzymes towards the harsher conditions often required for thermal and electrochemical catalysis.

*Molecular catalysis*

The modern molecular synthetic toolkit affords virtually unlimited scope for tailoring the primary, secondary, and outer coordination sphere around a molecular EAM active site. Several areas of exploration leverage this synthetic capability to embrace the unique physical properties of EAMs (Figure 5).
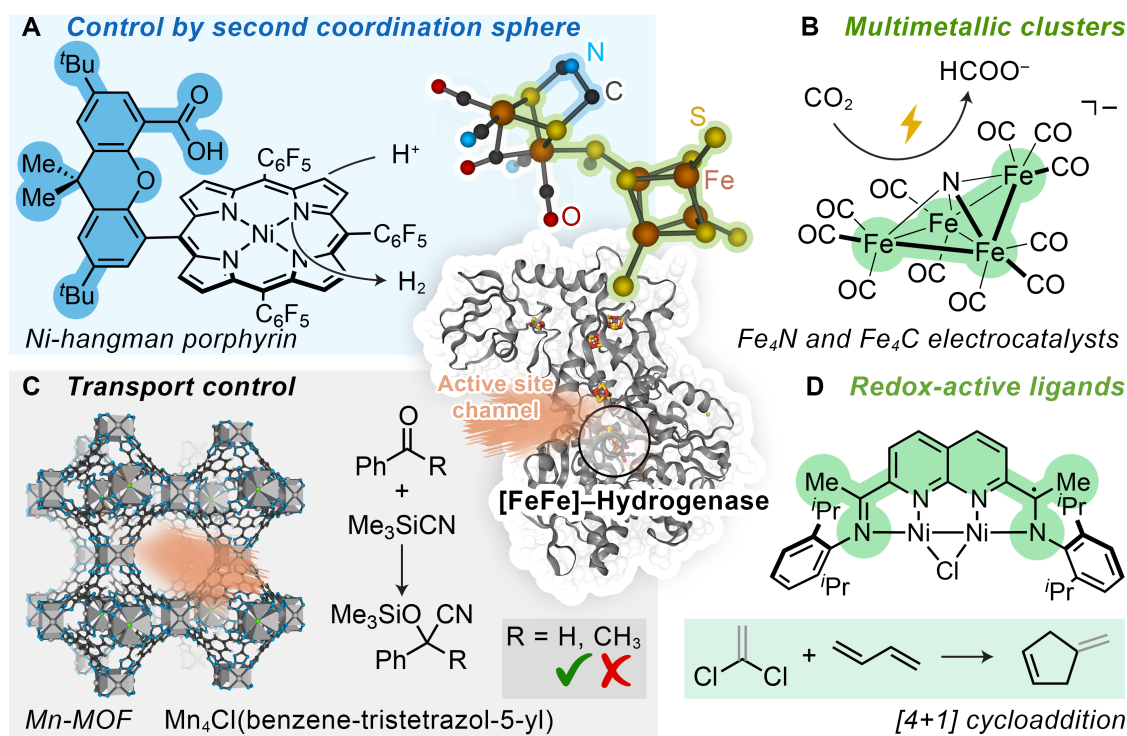
**Figure 5.** EAM enzymes such as [Fe-Fe]-hydrogenase (center) provide the blueprint for molecular EAM catalyst design. (A) Proton relays positioned proximate to EAM actives sites (blue highlight) are deployed in molecular catalysts for hydrogen production.(*57*) (B) Multi-metallic cluster active sites catalyze energy conversion reactions.(*58*) (C) Transport to active sites via enzyme channels can be mimicked in porous molecular materials.(*59*) (D) The density of available electronic states is increased through redox-active ligands that can steer reactivity in synthetic systems.(*60*)

EAM active sites in nature are subject to exquisite tuning by the arrangement of proximal amino acid residues and cofactors, as well as by the enzyme channels that gate the transport of reactants and products in and out. Similarly, achieving precise control over the local environment and transport in synthetic molecular EAM catalysts is critical for realizing their full potential. The ability to synthesize increasingly sophisticated ligands provides control of steric and electronic attributes, as demonstrated by remarkable progress in asymmetric hydrogenations, which are used extensively for enantioselective reactions required in the preparation of pharmaceuticals and agrochemicals. This field has been dominated by Rh- and Ru-based catalysts with chiral diphosphines,(*61*) but recent examples show that EAM catalysts can offer outstanding selectivity. For example, an Fe complex(*62*) catalyzes the asymmetric transfer hydrogenation of ketones with performance superior to that of Ru catalysts, and a Co complex catalyzes the asymmetric hydrogenation of the C=C bond of enamides.(*63*)

In addition to modifications of the ligands bound directly to the metal (primary coordination sphere), the environment of molecular catalysts can be tuned by positioning secondary coordination sphere substituents, such as Lewis acids,(*64*) positively charged groups,(*65-67*) hydrogen bond donors,(*68*) and pendant amines functioning as proton relays(*69-73*) (Figure 5A) proximal to the EAM center. These strategies have enhanced the rates of molecular EAM catalysis of electrochemical H$_2$ evolution,(*69-71*) H$_2$ oxidation,(*70, 71, 73*) CO$_2$ reduction,(*65*) and O$_2$ reduction.(*74*) Since the redox reactivity involves coupling of electron flow and bond

11

rearrangement, the secondary sphere substituents must be precisely positioned to foster optimal cooperativity. For example, the rates of proton-coupled electron transfer(*75, 76*) can be sensitive to sub-angstrom level changes in the proton-donor acceptor distance.(*77*) Cooperativity between the primary and secondary spheres in enzymes is achieved through the dynamic flexibility of the protein scaffold,(*26*) a property that is difficult to recreate systematically in synthetic EAM catalysts. Strong electric fields can influence enzyme catalysis(*78*) by manipulating the energies of intermediates or transition states, changing the rates and selectivity. Computations offer the opportunity to pre-screen the impact of positioning of the secondary sphere moieties; such studies could motivate synthetic efforts towards optimized secondary sphere control in EAM catalysis.

Controlling transport to EAM active sites is difficult to achieve with freely diffusing small molecules, but unique transport environments can be created by anchoring molecular EAM active sites on the surfaces of, or within the pores of, extended solid host materials including, for example, graphitic carbon, microporous silica, and metal-organic frameworks (MOFs).(*79*) Solid-supported site-isolated EAMs have been employed to catalyze a wide array of reactions; they benefit from structural constraints that prevent inhibitory bimolecular reactivity between metal centers, as well as facile catalyst separation and recycling. For these molecular materials, the extended lattice can serve as scaffolding to incorporate secondary sphere elements proximate to the embedded active site, and the pore structure and dimensions can be used to gate the transport of reactant and products to and from the active site. MOFs with EAM active sites have been deployed to carry out, for example, photocatalytic $CO_2$ reduction,(*80*) ethylene hydrogenation,(*81*) oxidation of alcohols,(*82*) olefin cyclopropanation,(*83*) arene C-H borylation,(*84*) tandem oxidation and functionalization of styrene,(*85*) and selective oxidation of methane to methanol.(*86*) Enzymes often feature disparate channels that transport of each reactant and product molecule in different directions, with the EAM active sites precisely positioned at the junction of these conduits. Similar precision has been difficult to achieve in synthetic systems, and efforts towards constructing molecular materials with actives sites at the intersection of multiple transport conduits could significantly advance selectivity in EAM catalysis.

Because of their low field strengths, EAM complexes have a propensity to undergo single-electron transfer pathways.(*87*) The control levers noted above are particularly important for embracing and controlling radical reactivity. Because of their smaller d-orbital splitting and weaker spin pairing energy, EAMs tend to react in enzymes through radical intermediates. Controlled radical reactions are central to biological detoxification by heme centers in cytochrome P450 enzymes, the synthesis of DNA precursors mediated by ribonucleotide reductase, and many other critical transformations mediated by cobalamins and radical SAM enzymes.(*10*) By controlling the reactivity of Co(III) carbon-centered radicals generated from Co(II) porphyrin complexes, ring closing reactions generated eight-membered rings, providing attractive synthetic methods for reactions that traditionally required precious metal catalysts.(*88*) Cooperative catalysis using EAM complexes of two metals, Ti and Cr, provided a highly selective route to anti-Markovnikov alcohols through ring-opening of epoxides.(*89*) This hydrogenation of epoxides is unusual since at different steps of the mechanism, a chromium complex transfers an electron, a hydrogen atom, and a proton.

Aerobic oxidation of primary alcohols to aldehydes and $H_2O_2$ is catalyzed in natural systems by galactose oxidase, a copper-containing enzyme. A bio-inspired synthetic binuclear copper complex exhibiting metal-ligand cooperative reactivity catalyzes the oxidation of primary alcohols using $O_2$ from air.(*90*) Similar to the accepted mechanism for galactose oxidase, the rate-

determining step of the synthetic system is proposed to involve hydrogen atom transfer from a C-H bond of the alcohol to the oxygen-centered radical bound to Cu.

Many of the EAM active sites that occur naturally, particularly those carrying out multi-electron redox transformations, feature multiple metal centers linked to each other in cluster active sites or metal centers coupled to redox-active cofactor ligands. The presence of these additional metals and redox-active ligands expands the number of available redox states accessible over a range of potentials. This increased density of electron states serves to buffer redox changes at the metal center that binds and activates the reactant, thereby lowering the energy barrier to multi-electron transformations. Harnessing the full power of EAMs in synthetic catalysts will require mastering the interactions of EAM centers with both metal-based and organic-based redox active ligands.

EAMs with redox-active ligands(*91-93*) catalyze a wide variety of reactions, including cleavage of C-C bonds,(*94*) cycloadditions,(*60*) oxidation of alcohols,(*95*) and aminations.(*96*) Further systematic deployment of redox-active ligands in EAM catalysis will benefit from general design rules for independently tuning metal-based and ligand-based redox levels to control the thermochemistry of elementary reaction steps. These ligands also play a key role in electrocatalysis at molecular active sites by providing a reservoir for accumulating redox equivalents that are cumulatively discharged to promote multi-electron reactions including, for example, $CO_2$ reduction,(*97*) and $O_2$ reduction.(*98*) An improved understanding of how to design systems with enhanced metal/ligand redox cooperativity would facilitate the design of more efficient (electro)catalysts.

Coupling between the metal binding site and another metal(s) can also increase the density of electronic states available for a multi-electron transformation. Bimetallic and multi-metallic EAM catalysts have been used for $CO_2$ reduction (Figure 5B),(*58, 99*) cycloadditions (Figure 5D) (*60*) dehydrogenation of formic acid,(*100*) and reduction of $NO_2$(*72*) or $O_2$.(*101*) Further systematic development of multi-metallic systems in EAM catalysis will benefit from a better understanding of how to stabilize the cluster against irreversible fragmentation while retaining the capacity to rapidly break and regenerate M-M or M-E-M (E = S, O) bonds during a catalytic cycle.

Understanding molecular EAM catalysts in systems with an increased density of states requires new spectroscopic tools and computational methods.(*102*) Whereas current computational methods effectively model weakly correlated closed-shell singlets, new methods are needed for accurately modeling open-shell species, and deconvolution of spin-state populations is required to accurately model the multi-configurational electronic structure of metal clusters and metal complex involving redox-active ligands.(*103*) Open-shell systems are often paramagnetic and intractable to characterize by routine NMR methods; emerging improved spectroscopic tools for characterizing paramagnetic species are advancing mechanistic understanding of these systems.(*104-106*)

*Heterogeneous catalysis*

Heterogeneous catalysis occurs on the surfaces of extended solids. While these extended solids may bear little direct structural resemblance to active sites in nature, the principles that define EAM catalysis in enzymes provide valuable leads towards their greater utility in heterogeneous catalysis.
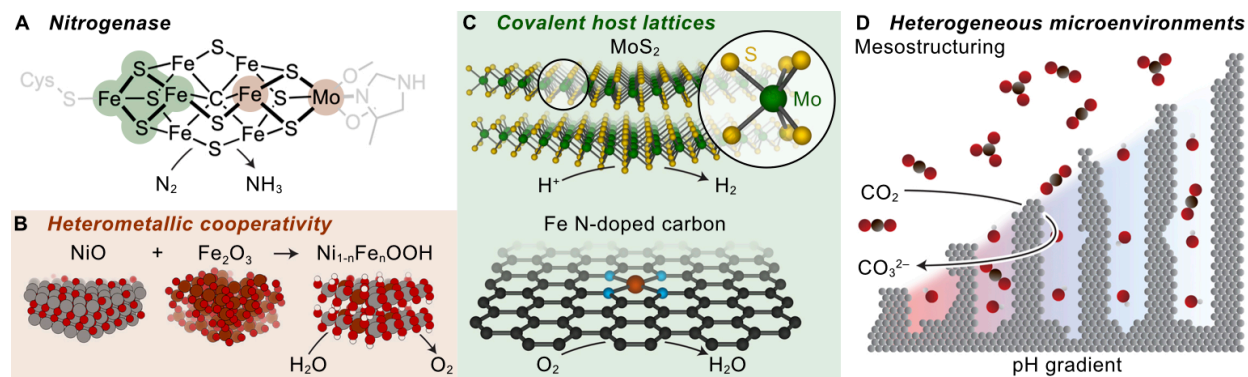
**Figure 6.** EAM sites in enzymes such as nitrogenase (A) provide the blueprint for heterogeneous EAM catalyst design. Multi-metallic cooperativity in nature (green in A) can guide the design of mixed metal-oxide oxygen evolution catalysts (B)(*107*). The more covalent metal-ligand bonding in natural systems (Fe/Mo in A) parallels the more covalent chalcogenide(*108*) and graphitic carbon host lattices(*109*) in synthetic catalysts (C). The function of the fine-tuned catalyst microenvironments in enzymes can be replicated in synthetic catalysts through micro- and meso-structuring. (D)(*110*)

Similar to the catalytic cooperativity in nature, enhanced catalytic performance can emerge from extended solids that incorporate multiple EAMs acting cooperatively. For example, by combining the different binding strength of Ti and Cu toward hydrogen, alloying Ti and Cu leads to hydrogen evolution reactivity similar to that of PGMs.(*111*) Analogously, mixed oxyhydroxides containing Fe, Co, and W catalyze oxygen evolution in an alkaline environment;(*112*) the cooperative interactions of even trace amounts of Fe can profoundly promote oxygen evolution activity on NiOOH (Figure 6B).(*113*) Considering the inherent lability of EAMs, improved characterization tools are needed to track the time-dependence of surface restructuring in multi-metallic EAM catalysts. Additionally, multi-metallic EAM oxide-based catalytic materials are challenging to model with conventional computational methods;(*114*) detailed mechanistic understanding of these systems would benefit from new computational tools that effectively model compositional heterogeneity and extend multi-configurational methods to periodic solids. Given the enormous compositional diversity available in multi-metallic solids, machine learning tools offer the potential to explore multi-dimensional reaction landscapes rapidly.

Historically, EAM heterogeneous catalysis focused predominantly on the reactivity of metal or metal oxide phases, the two endpoint thermodynamic sinks under reducing or oxidizing conditions, respectively. In contrast, many EAM active sites in nature are hosted within highly evolved combinations of sulfur, nitrogen, and carbon in the primary coordination environments, suggesting an appealing opportunity to exploit new types of heterogeneous catalysts. Relative to the O atoms in oxide host lattices, the greater orbital extension and/or energetic match of the p-orbitals in C, N, P, and S with the d-orbitals of EAMs leads to dramatic changes in the band structures of chalcogenides,(*108, 115*) pnictides,(*116*)·(*117, 118*) and carbides,(*116, 119*) potentially endowing these EAM catalysts with enhanced activity relative to the corresponding metal or oxide phases. For example, metal sulfide and phosphide materials have emerged as potent catalysts for electrochemical hydrogen evolution,(*115*) and EAM carbides have been shown to be highly selective for hydrodeoxygenation of biomass-derived molecules.(*120*) Considering the vast phase space available among chalcogenides, pnictides, and carbides, there is ample opportunity to

discover new EAM catalysts that take advantage of environments akin to those found in nature. Progress towards these goals will require advances in the synthesis of materials with tunable phase and nanostructure at sufficient scales for catalytic applications. In addition, since these materials are typically metastable relative to their corresponding metal or oxide phases, fundamental insights are needed to understand how the surfaces of these materials undergo reconstruction under sustained catalytic turnover.(*121*) Surface-sensitive operando spectroscopic characterization(*122*) revealing the chemical stability of these materials is critical for the design of optimal catalysis.

EAM active sites can also be hosted within graphitic carbon host lattices. For many decades, it has been recognized that the high-temperature pyrolysis of nitrogen and carbon precursors bound to EAMs such as Fe and Co can lead to the generation of relatively high-performance electrocatalysts for the oxygen reduction reaction in fuel cells.(*123, 124*) These materials, often referred to as M-N-C catalysts, are postulated to contain metal nanoparticles and mononuclear metal sites embedded in the graphitic framework, with varying ratios depending on the synthetic conditions.(*125*) Fe-N-C materials are leading EAM candidates to replace Pt in fuel cells and this class of materials presents a unique opportunity to create emergent reactivity from EAMs through strong interaction between the EAM orbitals and the electronic states of graphitic carbons. Despite decades of work in this area, the local structure of the active sites remains poorly understood, and the synthetic toolkit for tuning the population of active sites remains limited. Thus, continued progress in this area will hinge on new strategies for better understanding and controlling the inherent distribution of active site structures present in these materials.

The microenvironment around the active site in natural systems is precisely controlled by pre-organizing reactants, imposing a local electric field, and controlling transport to and from active sites. The dynamic nature of EAMs affords opportunities to implement these concepts within heterogeneous catalysts. Many strategies have been employed for imposing a unique microenvironment at the catalyst surface – for catalysis at solid-liquid interfaces, the composition of the solvent or electrolyte can be varied; the catalyst can be designed with appropriate meso/microstructure to create diffusional gradients at the surface; and the catalyst surface can be chemically modified.(*126*) Electrolyte choice, catalyst mesostructuring, and chemical modification have all been applied to tune the selectivity of Cu-based $CO_2$/CO reduction catalysts.(*127*) The solution environment can also be used to favor mechanisms for dynamic self-repair of catalysts; for example, Co ions in solution promote dynamic stability and self-repair of Co-based oxygen evolution catalysts that would otherwise undergo corrosion.(*128*) Additionally, thin gas-permeable layers of ionic liquids(*129*) and/or molecular promoters could create unique microenvironments that contain substrate binding units proximate to active sites. This strategy enhances the stability of EAMs prone to irreversible reconstruction/oxidation, and may also foster improved selectivity. Despite the enormous synthetic opportunities in this area, mechanistic insights into how local microenvironments tune heterogeneous catalysis are rare. Although there are many tools for operando characterization of catalysts, these tools often only shed light on the primary coordination environments of EAM active sites. Thus, improved tools are needed for characterizing longer-range interactions in the secondary and outer coordination spheres that define the microenvironment of the catalyst. Notwithstanding these formidable challenges, the tantalizing prospect of creating enzyme-like three-dimensional active sites on surfaces has enormous appeal for emerging EAM catalysis.

**Outlook**
While recent years have seen tremendous growth in both the development and application of EAM catalysts, the fundamental understanding of reactivity patterns of these metals has lagged behind that of PGMs. This disparity in both understanding and use of EAMs is attributed to the broader landscape of reactivity available to EAMs and the smaller historical investment devoted to the study of them. The gaps in fundamental scientific knowledge highlighted here are intended as a "call to action" to identify and overcome scientific barriers to EAM catalysis, based on compelling opportunities that embrace and exploit the characteristic reactivity of EAMs. Examples of recent discoveries of EAM catalysts that rival, or even exceed, the performance of PGM catalysts document the value of identifying design principles for new classes of catalysts. In addition to catalytic activity, EAM catalysts should possess long-term stability and high volume site density for practical applications. The quest to develop efficient, sustainable catalysts based on EAMs benefits from cohesive efforts in synthesis, operando characterization, mechanistic inquiry, materials design, and theoretical modeling. Spurred by recent advances, the collective efforts of the catalysis community can bring the full potential of EAM catalysts to be realized.

**Competing Interests**: The authors have no competing interests relevant to this publication.

**References**
1. *CRC Handbook of Chemistry and Physics, 97th Edition*.  (2016-2017).
2. P. Nuss, M. J. Eckelman, Life Cycle Assessment of Metals: A Scientific Synthesis. *PLOS ONE* **9**, e101298 (2014).
3. J. Liu *et al.*, Metalloproteins Containing Cytochrome, Iron–Sulfur, or Copper Redox Centers. *Chem. Rev.* **114**, 4366-4469 (2014).
4. M. A. Thorseth, C. E. Tornow, E. C. M. Tse, A. A. Gewirth, Cu complexes that catalyze the oxygen reduction reaction. *Coord. Chem. Rev.* **257**, 130-139 (2013).
5. E. I. Solomon *et al.*, Copper Active Sites in Biology. *Chem. Rev.* **114**, 3659-3853 (2014).
6. L. C. Seefeldt *et al.*, Energy Transduction in Nitrogenase. *Acc. Chem. Res.* **51**, 2179-2186 (2018).
7. W. Lubitz, H. Ogata, O. Rüdiger, E. Reijerse, Hydrogenases. *Chem. Rev.* **114**, 4081-4148 (2014).
8. J. P. McEvoy, G. W. Brudvig, Water-Splitting Chemistry of Photosystem II. *Chem. Rev.* **106**, 4455-4483 (2006).
9. V. C. C. Wang *et al.*, Alkane Oxidation: Methane Monooxygenases, Related Enzymes, and Their Biomimetics. *Chem. Rev.* **117**, 8574-8621 (2017).
10. J. B. Broderick, B. R. Duffus, K. S. Duschene, E. M. Shepard, Radical *S*-Adenosylmethionine Enzymes. *Chem. Rev.* **114**, 4229-4317 (2014).
11. C. C. C. Johansson Seechurn, M. O. Kitching, T. J. Colacot, V. Snieckus, Palladium-Catalyzed Cross-Coupling: A Historical Contextual Perspective to the 2010 Nobel Prize. *Angew. Chem. Int. Ed.* **51**, 5062-5085 (2012).

12. R. Dorel, C. P. Grugel, A. M. Haydl, The Buchwald–Hartwig Amination After 25 Years. *Angew. Chem. Int. Ed.* **58**, 17118-17129 (2019).

13. R. Franke, D. Selent, A. Börner, Applied Hydroformylation. *Chem. Rev.* **112**, 5675-5732 (2012).

14. J. K. Nørskov *et al.*, Trends in the Exchange Current for Hydrogen Evolution. *J. Electrochem. Soc.* **152**, J23-J26 (2005).

15. C. C. L. McCrory, S. Jung, J. C. Peters, T. F. Jaramillo, Benchmarking Heterogeneous Electrocatalysts for the Oxygen Evolution Reaction. *J. Am. Chem. Soc.* **135**, 16977-16987 (2013).

16. J. F. Hartwig, Evolution of C–H Bond Functionalization from Methane to Methodology. *J. Am. Chem. Soc.* **138**, 2-24 (2016).

17. R. E. Smalley, Future Global Energy Prosperity: The Terawatt Challenge. *MRS Bull.* **30**, 412-417 (2005).

18. P. C. K. Vesborg, T. F. Jaramillo, Addressing the terawatt challenge: scalability in the supply of chemical elements for renewable energy. *RSC Adv.* **2**, 7933-7947 (2012).

19. K. S. Egorova, V. P. Ananikov, Toxicity of Metal Compounds: Knowledge and Myths. *Organometallics* **36**, 4071-4090 (2017).

20. J. D. Hayler, D. K. Leahy, E. M. Simmons, A Pharmaceutical Industry Perspective on Sustainable Metal Catalysis. *Organometallics* **38**, 36-46 (2019).

21. A. J. Medford *et al.*, From the Sabatier principle to a predictive theory of transition-metal heterogeneous catalysis. *J. Catal.* **328**, 36-42 (2015).

22. J. J. H. B. Sattler, J. Ruiz-Martinez, E. Santillan-Jimenez, B. M. Weckhuysen, Catalytic Dehydrogenation of Light Alkanes on Metals and Metal Oxides. *Chem. Rev.* **114**, 10613-10653 (2014).

23. K. M. Light, J. A. Wisniewski, W. A. Vinyard, M. T. Kieber-Emmons, Perception of the plant hormone ethylene: known-knowns and known-unknowns. *JBIC, J. Biol. Inorg. Chem.* **21**, 715-728 (2016).

24. H. S. Toogood, N. S. Scrutton, Discovery, Characterization, Engineering, and Applications of Ene-Reductases for Industrial Biocatalysis. *ACS Catal.* **8**, 3532-3549 (2018).

25. M. Costas, M. P. Mehn, M. P. Jensen, L. Que, Dioxygen Activation at Mononuclear Nonheme Iron Active Sites: Enzymes, Models, and Intermediates. *Chem. Rev.* **104**, 939-986 (2004).

26. G. G. Hammes, S. J. Benkovic, S. Hammes-Schiffer, Flexibility, Diversity, and Cooperativity: Pillars of Enzyme Catalysis. *Biochemistry* **50**, 10422-10430 (2011).

27. J. K. McCusker, Electronic structure in the transition metal block and its implications for light harvesting. *Science* **363**, 484-488 (2019).

28. P. Pyykko, Relativistic Effects in Structural Chemistry. *Chem. Rev.* **88**, 563-594 (1988).

29. L. A. Watson, O. V. Ozerov, M. Pink, K. G. Caulton, Four-Coordinate, Planar Ru(II). A Triplet State as a Response to a 14-Valence Electron Configuration. *J. Am. Chem. Soc.* **125**, 8426-8427 (2003).

30. M. Kinauer *et al.*, An iridium(III/IV/V) redox series featuring a terminal imido complex with triplet ground state. *Chem. Sci.* **9**, 4325-4332 (2018).

31. M. Swart, M. Costas, Eds., *Spin States in Biochemistry and Inorganic Chemistry: Influence on Structure and Reactivity*, (John Wiley & Sons, Chichester, UK, 2016).

32. D. P. Estes, A. K. Vannucci, A. R. Hall, D. L. Lichtenberger, J. R. Norton, Thermodynamics of the Metal-Hydrogen Bonds in $(\eta^5\text{-}C_5H_5)M(CO)_2H$ (M = Fe, Ru, Os). *Organometallics* **30**, 3444-3447 (2011).

33. J. Zhang, D. C. Grills, K.-W. Huang, E. Fujita, R. M. Bullock, Carbon-to-Metal Hydrogen Atom Transfer: Direct Observation Using Time-Resolved Infrared Spectroscopy. *J. Am. Chem. Soc.* **127**, 15684-15685 (2005).

34. V. D. Parker, K. L. Handoo, F. Roness, M. Tilset, Electrode Potentials and Thermodynamics of Isodesmic Reactions. *J. Am. Chem. Soc.* **113**, 7493-7498 (1991).

35. N. M. Marshall *et al.*, Rationally tuning the reduction potential of a single cupredoxin beyond the natural range. *Nature* **462**, 113 (2009).

36. A. B. P. Lever, Electrochemical Parametrization of Metal Complex Redox Potentials, Using the Ruthenium(III)/ruthenium(II) Couple to Generate a Ligand Electrochemical Series. *Inorg. Chem.* **29**, 1271-1285 (1990).

37. M. Wikström, K. Krab, V. Sharma, Oxygen Activation and Energy Conservation by Cytochrome *c* Oxidase. *Chem. Rev.* **118**, 2469-2490 (2018).

38. H. Falsig *et al.*, Trends in the Catalytic CO Oxidation Activity of Nanoparticles. *Angew. Chem. Int. Ed.* **47**, 4835-4839 (2008).

39. L. Helm, A. E. Merbach, Inorganic and Bioinorganic Solvent Exchange Mechanisms. *Chem. Rev.* **105**, 1923-1960 (2005).

40. C. A. Gaggioli, S. J. Stoneburner, C. J. Cramer, L. Gagliardi, Beyond Density Functional Theory: The Multiconfigurational Approach To Model Heterogeneous Catalysis. *ACS Catal.* **9**, 8481-8502 (2019).

41. P. Schlexer Lamoureux *et al.*, Machine Learning for Computational Heterogeneous Catalysis. *ChemCatChem* **11**, 3581-3601 (2019).

42. J. P. Janet, S. Ramesh, C. Duan, H. J. Kulik, Accurate Multiobjective Design in a Space of Millions of Transition Metal Complexes with Neural-Network-Driven Efficient Global Optimization. *ACS Cent. Sci.* **6**, 513-524 (2020).

43. B. Meyer, B. Sawatlon, S. Heinen, O. A. von Lilienfeld, C. Corminboeuf, Machine learning meets volcano plots: computational discovery of cross-coupling catalysts. *Chem. Sci.* **9**, 7069-7077 (2018).

44. Z. W. Ulissi *et al.*, Machine-Learning Methods Enable Exhaustive Searches for Active Bimetallic Facets and Reveal Active Site Motifs for $CO_2$ Reduction. *ACS Catal.* **7**, 6600-6608 (2017).

45. M. Zhong *et al.*, Accelerated discovery of $CO_2$ electrocatalysts using active machine learning. *Nature* **581**, 178-183 (2020).

46. K. Saravanan, J. R. Kitchin, O. A. von Lilienfeld, J. A. Keith, Alchemical Predictions for Computational Catalysis: Potential and Limitations. *J. Phys. Chem. Lett.* **8**, 5002-5007 (2017).

47. T. Bligaard *et al.*, Toward Benchmarking in Catalysis Science: Best Practices, Challenges, and Opportunities. *ACS Catal.* **6**, 2590-2602 (2016).

48. O. Khersonsky, D. S. Tawfik, Enzyme Promiscuity: A Mechanistic and Evolutionary Perspective. *Annu. Rev. Biochem.* **79**, 471-505 (2010).

49. H. M. L. Davies, D. Morton, Guiding principles for site selective and stereoselective intermolecular C–H functionalization by donor/acceptor rhodium carbenes. *Chem. Soc. Rev.* **40**, 1857-1869 (2011).

50.  O. F. Brandenberg, K. Chen, F. H. Arnold, Directed Evolution of a Cytochrome P450 Carbene Transferase for Selective Functionalization of Cyclic Compounds. *J. Am. Chem. Soc.* **141**, 8989-8995 (2019).

51.  R. K. Zhang *et al.*, Enzymatic assembly of carbon–carbon bonds via iron-catalysed sp$^3$ C–H functionalization. *Nature* **565**, 67-72 (2018).

52.  J. F. Hartwig, M. A. Larsen, Undirected, Homogeneous C–H Bond Functionalization: Challenges and Opportunities. *ACS Cent. Sci.* **2**, 281-292 (2016).

53.  O. F. Brandenberg, R. Fasan, F. H. Arnold, Exploiting and engineering hemoproteins for abiological carbene and nitrene transfer reactions. *Curr. Opin. Biotechnol.* **47**, 102-111 (2017).

54.  G. Jiménez-Osés *et al.*, The role of distant mutations and allosteric regulation on LovD active site dynamics. *Nat. Chem. Biol.* **10**, 431-436 (2014).

55.  F. Niehaus, C. Bertoldo, M. Kähler, G. Antranikian, Extremophiles as a source of novel enzymes for industrial application. *Appl. Microbiol. Biotechnol.* **51**, 711-729 (1999).

56.  A. M. Klibanov, Improving enzymes by using them in organic solvents. *Nature* **409**, 241-246 (2001).

57.  B. H. Solis, A. G. Maher, D. K. Dogutan, D. G. Nocera, S. Hammes-Schiffer, Nickel phlorin intermediate formed by proton-coupled electron transfer in hydrogen evolution mechanism. *Proc. Natl. Acad. Sci. U.S.A.* **113**, 485-492 (2016).

58.  N. D. Loewen, T. V. Neelakantan, L. A. Berben, Renewable Formate from C–H Bond Formation with $CO_2$: Using Iron Carbonyl Clusters as Electrocatalysts. *Acc. Chem. Res.* **50**, 2362-2370 (2017).

59.  S. Horike, M. Dincă, K. Tamaki, J. R. Long, Size-Selective Lewis Acid Catalysis in a Microporous Metal-Organic Framework with Exposed $Mn^{2+}$ Coordination Sites. *J. Am. Chem. Soc.* **130**, 5854-5855 (2008).

60.  Y.-Y. Zhou, C. Uyeda, Catalytic reductive [4 + 1]-cycloadditions of vinylidenes and dienes. *Science* **363**, 857-862 (2019).

61.  R. Noyori, Asymmetric Catalysis: Science and Opportunities (Nobel Lecture). *Angew. Chem., Int. Ed.* **41**, 2008-2022 (2002).

62.  W. Zuo, A. J. Lough, Y. Li, R. H. Morris, Amine(imine)diphosphines Activate Iron Catalysts in the Asymmetric Transfer Hydrogenation of Ketones and Imines *Science* **342**, 1080-1083 (2013).

63.  M. R. Friedfeld, H. Zhong, R. T. Ruck, M. Shevlin, P. J. Chirik, Cobalt-catalyzed asymmetric hydrogenation of enamides enabled by single-electron reduction. *Science* **360**, 888-893 (2018).

64.  J. J. Kiernicki, M. Zeller, N. K. Szymczak, Hydrazine Capture and N–N Bond Cleavage at Iron Enabled by Flexible Appended Lewis Acids. *J. Am. Chem. Soc.* **139**, 18194-18197 (2017).

65.  I. Azcarate, C. Costentin, M. Robert, J.-M. Savéant, Through-Space Charge Interaction Substituent Effects in Molecular Catalysis Leading to the Design of the Most Efficient Catalyst of $CO_2$-to-CO Electrochemical Conversion. *J. Am. Chem. Soc.* **138**, 16639-16644 (2016).

66.  T. Chantarojsiri, J. W. Ziller, J. Y. Yang, Incorporation of redox-inactive cations promotes iron catalyzed aerobic C-H oxidation at mild potentials. *Chem. Sci.* **9**, 2567-2574 (2018).

67. D. J. Martin, B. Q. Mercado, J. M. Mayer, Combining scaling relationships overcomes rate versus overpotential trade-offs in $O_2$ molecular electrocatalysis. *Sci. Adv.* **6**, eaaz3318 (2020).

68. C. L. Ford, Y. J. Park, E. M. Matson, Z. Gordon, A. R. Fout, A bioinspired iron catalyst for nitrate and perchlorate reduction. *Science* **354**, 741-743 (2016).

69. C. M. Klug, A. Cardenas, R. M. Bullock, M. O'Hagan, E. S. Wiedner, Reversing the Tradeoff Between Rate and Overpotential in Molecular Electrocatalysts for $H_2$ Production. *ACS Catal.* **8**, 3286–3296 (2018).

70. A. Le Goff *et al.*, From Hydrogenases to Noble Metal–Free Catalytic Nanomaterials for $H_2$ Production and Uptake. *Science* **326**, 1384-1387 (2009).

71. T. N. Huan *et al.*, Bio-inspired noble metal-free nanomaterials approaching platinum performances for $H_2$ evolution and uptake. *Energy Environ. Sci.* **9**, 940-947 (2016).

72. C.-W. Hsu, S. C. Rathnayaka, S. M. Islam, S. N. MacMillan, N. P. Mankad, $N_2O$ Reductase Activity of a [$Cu_4S$] Cluster in the $4Cu^I$ Redox State Modulated by Hydrogen Bond Donors and Proton Relays in the Secondary Coordination Sphere. *Angew. Chem. Int. Ed.* **59**, 627-631 (2020).

73. T. Liu, D. L. DuBois, R. M. Bullock, An iron complex with pendent amines as a molecular electrocatalyst for oxidation of hydrogen. *Nat. Chem.* **5**, 228-233 (2013).

74. D. J. Martin, B. Q. Mercado, J. M. Mayer, Combining scaling relationships overcomes rate vs. overpotential tradeoffs in $O_2$ molecular electrocatalysis. *Sci. Adv.*, aaz3318, in press. (2020).

75. J. J. Warren, T. A. Tronic, J. M. Mayer, Thermochemistry of Proton-Coupled Electron Transfer Reagents and its Implications. *Chem. Rev.* **110**, 6961-7001 (2010).

76. D. R. Weinberg *et al.*, Proton-Coupled Electron Transfer. *Chem. Rev.* **112**, 4016-4093 (2012).

77. S. Horvath, L. E. Fernandez, A. V. Soudackov, S. Hammes-Schiffer, Insights into proton-coupled electron transfer mechanisms of electrocatalytic $H_2$ oxidation and production. *Proc. Natl. Acad. Sci. U.S.A.* **109**, 15663-15668 (2012).

78. S. D. Fried, S. Bagchi, S. G. Boxer, Extreme electric fields power catalysis in the active site of ketosteroid isomerase. *Science* **346**, 1510-1514 (2014).

79. Q. Wang, D. Astruc, State of the Art and Prospects in Metal–Organic Framework (MOF)-Based and MOF-Derived Nanocatalysis. *Chem. Rev.* **120**, 1438-1511 (2020).

80. X. Feng *et al.*, Metal–Organic Frameworks Significantly Enhance Photocatalytic Hydrogen Evolution and $CO_2$ Reduction with Earth-Abundant Copper Photosensitizers. *J. Am. Chem. Soc.* **142**, 690-695 (2020).

81. J. Liu *et al.*, Introducing Nonstructural Ligands to Zirconia-like Metal–Organic Framework Nodes To Tune the Activity of Node-Supported Nickel Catalysts for Ethylene Hydrogenation. *ACS Catal.* **9**, 3198-3207 (2019).

82. K.-i. Otake *et al.*, Single-Atom-Based Vanadium Oxide Catalysts Supported on Metal–Organic Frameworks: Selective Alcohol Oxidation and Structure–Activity Relationship. *J. Am. Chem. Soc.* **140**, 8652-8656 (2018).

83. C. Sun, G. Skorupskii, J.-H. Dou, A. M. Wright, M. Dincă, Reversible Metalation and Catalysis with a Scorpionate-like Metallo-ligand in a Metal–Organic Framework. *J. Am. Chem. Soc.* **140**, 17394-17398 (2018).

84. T. Zhang, K. Manna, W. Lin, Metal–Organic Frameworks Stabilize Solution-Inaccessible Cobalt Catalysts for Highly Efficient Broad-Scope Organic Transformations. *J. Am. Chem. Soc.* **138**, 3241-3249 (2016).

85. M. H. Beyzavi *et al.*, A Hafnium-Based Metal–Organic Framework as a Nature-Inspired Tandem Reaction Catalyst. *J. Am. Chem. Soc.* **137**, 13624-13631 (2015).

86. J. Baek *et al.*, Bioinspired Metal–Organic Framework Catalysts for Selective Methane Oxidation to Methanol. *J. Am. Chem. Soc.* **140**, 18208-18216 (2018).

87. N. P. van Leest *et al.*, in *Adv. Organomet. Chem.*, P. J. Pérez, F. G. A. Stone, R. West, Eds. (Academic Press, 2018), vol. 70, chap. 2, pp. 71-180.

88. C. te Grotenhuis, N. van den Heuvel, J. I. van der Vlugt, B. de Bruin, Catalytic Dibenzocyclooctene Synthesis via Cobalt(III)–Carbene Radical and ortho-Quinodimethane Intermediates. *Angew. Chem. Int. Ed.* **57**, 140-145 (2018).

89. C. Yao, T. Dahmen, A. Gansäuer, J. Norton, Anti-Markovnikov alcohols via epoxide hydrogenation through cooperative catalysis. *Science* **364**, 764-767 (2019).

90. P. Chaudhuri, M. Hess, U. Flörke, K. Wieghardt, From Structural Models of Galactose Oxidase to Homogeneous Catalysis: Efficient Aerobic Oxidation of Alcohols. *Angew. Chem. Int. Ed.* **37**, 2217-2220 (1998).

91. P. J. Chirik, K. Wieghardt, Radical Ligands Confer Nobility on Base-Metal Catalysts. *Science* **327**, 794-795 (2010).

92. V. K. K. Praneeth, M. R. Ringenberg, T. R. Ward, Redox-Active Ligands in Catalysis. *Angew. Chem. Int. Ed.* **51**, 10228-10234 (2012).

93. V. Lyaskovskyy, B. de Bruin, Redox Non-Innocent Ligands: Versatile New Tools to Control Catalytic Reactions. *ACS Catal.* **2**, 270-279 (2012).

94. J. M. Darmon *et al.*, Oxidative Addition of Carbon–Carbon Bonds with a Redox-Active Bis(imino)pyridine Iron Complex. *J. Am. Chem. Soc.* **134**, 17125-17137 (2012).

95. L. Que, W. B. Tolman, Biologically inspired oxidation catalysis. *Nature* **455**, 333-340 (2008).

96. K. M. Carsch *et al.*, Synthesis of a copper-supported triplet nitrene complex pertinent to copper-catalyzed amination. *Science* **365**, 1138-1143 (2019).

97. C. Römelt *et al.*, Electronic Structure of a Formal Iron(0) Porphyrin Complex Relevant to $CO_2$ Reduction. *Inorg. Chem.* **56**, 4745-4750 (2017).

98. C. J. Kaminsky, J. Wright, Y. Surendranath, Graphite-Conjugation Enhances Porphyrin Electrocatalysis. *ACS Catal.* **9**, 3667-3671 (2019).

99. R. B. Ferreira, L. J. Murray, Cyclophanes as Platforms for Reactive Multimetallic Complexes. *Acc. Chem. Res.* **52**, 447-455 (2019).

100. T. Nakajima *et al.*, Synergistic $Cu_2$ Catalysts for Formic Acid Dehydrogenation. *J. Am. Chem. Soc.* **141**, 8732-8736 (2019).

101. S. Dey *et al.*, Electrocatalytic $O_2$ Reduction by [Fe-Fe]-Hydrogenase Active Site Models. *J. Am. Chem. Soc.* **136**, 8847-8850 (2014).

102. S. Sharma, K. Sivalingam, F. Neese, G. K.-L. Chan, Low-energy spectrum of iron–sulfur clusters directly from many-particle quantum mechanics. *Nat. Chem.* **6**, 927 (2014).

103. L. Gagliardi *et al.*, Multiconfiguration Pair-Density Functional Theory: A New Way To Treat Strongly Correlated Systems. *Acc. Chem. Res.* **50**, 66-73 (2017).

104. J. C. Ott, H. Wadepohl, M. Enders, L. H. Gade, Taking Solution Proton NMR to Its Extreme: Prediction and Detection of a Hydride Resonance in an Intermediate-Spin Iron Complex. *J. Am. Chem. Soc.* **140**, 17413−17417 (2018).

105. P. L. Holland, Distinctive Reaction Pathways at Base Metals in High-Spin Organometallic Catalysts. *Acc. Chem. Res.* **48**, 1696-1702 (2015).

106. M. P. Crockett, H. Zhang, C. M. Thomas, J. A. Byers, Adding diffusion ordered NMR spectroscopy (DOSY) to the arsenal for characterizing paramagnetic complexes. *Chem. Commun.* **55**, 14426-14429 (2019).

107. L. Trotochaud, S. L. Young, J. K. Ranney, S. W. Boettcher, Nickel-Iron Oxyhydroxide Oxygen-Evolution Electrocatalysts: The Role of Intentional and Incidental Iron Incorporation. *J. Am. Chem. Soc.* **136**, 6744 (2014).

108. T. F. Jaramillo *et al.*, Identification of Active Edge Sites for Electrochemical $H_2$ Evolution from $MoS_2$ Nanocatalysts. *Science* **317**, 100-102 (2007).

109. F. Jaouen *et al.*, Recent advances in non-precious metal catalysis for oxygen-reduction reaction in polymer electrolyte fuel cells. *Energy Environ. Sci.* **4**, 114-130 (2011).

110. R. Kas *et al.*, Electrochemical $CO_2$ reduction on nanostructured metal electrodes: fact or defect? *Chem. Sci.* **11**, 1738-1749 (2020).

111. Q. Lu *et al.*, Highly porous non-precious bimetallic electrocatalysts for efficient hydrogen evolution. *Nat. Commun.* **6**, 6567 (2015).

112. B. Zhang *et al.*, Homogeneously dispersed multimetal oxygen-evolving catalysts. *Science* **352**, 333-337 (2016).

113. L. Trotochaud, S. L. Young, J. K. Ranney, S. W. Boettcher, Nickel–Iron Oxyhydroxide Oxygen-Evolution Electrocatalysts: The Role of Intentional and Incidental Iron Incorporation. *J. Am. Chem. Soc.* **136**, 6744-6753 (2014).

114. E. A. Carter, Challenges in Modeling Materials Properties Without Experimental Input. *Science* **321**, 800-803 (2008).

115. Z. W. Seh *et al.*, Combining theory and experiment in electrocatalysis: Insights into materials design. *Science* **355**, eaad4998 (2017).

116. J. G. Chen, Carbide and Nitride Overlayers on Early Transition Metal Surfaces: Preparation, Characterization, and Reactivities. *Chem. Rev.* **96**, 1477-1498 (1996).

117. Z. W. Seh *et al.*, Two-Dimensional Molybdenum Carbide (MXene) as an Efficient Electrocatalyst for Hydrogen Evolution. *ACS Energy Lett.* **1**, 589-594 (2016).

118. J. Kibsgaard *et al.*, Designing an improved transition metal phosphide catalyst for hydrogen evolution using experimental and theoretical trends. *Energy Environ. Sci.* **8**, 3022-3029 (2015).

119. R. B. Levy, M. Boudart, Platinum-Like Behavior of Tungsten Carbide in Surface Catalysis. *Science* **181**, 547-549 (1973).

120. Z. Lin, R. Chen, Z. Qu, J. G. Chen, Hydrodeoxygenation of biomass-derived oxygenates over metal carbides: from model surfaces to powder catalysts. *Green Chem.* **20**, 2679-2696 (2018).

121. B. Yan *et al.*, Surface Restructuring of Nickel Sulfide Generates Optimally Coordinated Active Sites for Oxygen Reduction Catalysis. *Joule* **1**, 600-612 (2017).

122. J. Dou *et al.*, Operando chemistry of catalyst surfaces during catalysis. *Chem. Soc. Rev.* **46**, 2001-2027 (2017).

123. G. Wu, P. Zelenay, Nanostructured Nonprecious Metal Catalysts for Oxygen Reduction Reaction. *Acc. Chem. Res.* **46**, 1878-1889 (2013).

124. Y. P. Zhu, C. Guo, Y. Zheng, S.-Z. Qiao, Surface and Interface Engineering of Noble-Metal-Free Electrocatalysts for Efficient Energy Conversion Processes. *Acc. Chem. Res.* **50**, 915-923 (2017).

125. T. Asset, P. Atanassov, Iron-Nitrogen-Carbon Catalysts for Proton Exchange Membrane Fuel Cells. *Joule* **4**, 33-44 (2020).
126. J. D. A. Pelletier, J.-M. Basset, Catalysis by Design: Well-Defined Single-Site Heterogeneous Catalysts. *Acc. Chem. Res.* **49**, 664-677 (2016).
127. S. Nitopi *et al.*, Progress and Perspectives of Electrochemical $CO_2$ Reduction on Copper in Aqueous Electrolyte. *Chem. Rev.* **119**, 7610-7672 (2019).
128. Y. Surendranath, D. A. Lutterman, Y. Liu, D. G. Nocera, Nucleation, Growth, and Repair of a Cobalt-Based Oxygen Evolving Catalyst. *J. Am. Chem. Soc.* **134**, 6326-6336 (2012).
129. J. M. Marinkovic, A. Riisager, R. Franke, P. Wasserscheid, M. Haumann, Fifteen Years of Supported Ionic Liquid Phase-Catalyzed Hydroformylation: Material and Process Developments. *Ind. Eng. Chem. Res.* **58**, 2409-2420 (2019).